COMPUTER VISION FOR REAL-TIME RELATIVE NAVIGATION WITH A NON-COOPERATIVE AND SPINNING TARGET SPACECRAFT

Setareh Yazdkhasti, Steve Ulrich, and Jurek Z. Sasiadek

Carleton University, Ottawa, Ontario, K1S 5B6, Canada

ABSTRACT

Relative navigation for spacecraft has received a great attention recently because of its importance for space applications. Many space missions require accurate relative position knowledge between space vehicles. This paper proposes a vision-based relative navigation system only based on stereo gray-scale camera. An effective Image processing algorithms was developed for estimating the relative position between non-cooperative, and spinning space objects. The experimental test-bed was used for the simulations of service missions of satellites to test the performance of the developed vision and navigation algorithms. Simulation results in a dark room with spinning scaled model of spacecraft, demonstrated the effectiveness of the proposed algorithm.

Key words: Uncooperative spacecraft; Stereo camera; Image processing.

1. INTRODUCTION

In reality, a majority of the failure satellites are spinning or tumbling in an orbit without light beacons and available state information which called non-cooperative satellites. When the satellites are non-cooperative, without available interactions between non-cooperative vehicles, the problem of relative state estimation becomes more complicated. Thus, the pose determination of a non-cooperative satellite becomes a tremendous challenge. Over the last decade, vision-based navigation systems have been extensively used to address the problem of relative motion determination, due to their low cost, mass, and power requirements, compared to active sensor-based techniques (e.g., laser range finder) [1]-[2]. Various researchers have investigated on pose estimation of an object and some of these techniques use vision-based sensors for measuring the motion of targets in the space environment. Their methods vary depending on their research objectives and assumptions. In particular, laboratory experimentations of cooperative vision-based navigation systems relying on known fiducial markers installed on the target vehicle were recently reported by Romano et al.[3] at the Naval Postgraduate School, and Tweddle and Saenz-Otero [4] at the Massachusetts Institute of Technology (MIT). Such cooperative vision systems were also extensively used on actual on-orbit missions. For example, the Space Vision System (SVS) [5] monitored and tracked a pattern of special dots installed on the International Space Station. As the Space Station moved, the system tracked the changing position of the dots, and calculated the relative motion between the two vehicles. However, when the target object has no fiducial markers, such vision systems cannot be used. It is therefore required to develop a strategy that does not rely on such markers, i.e., a relative navigation system applicable for unknown, uncooperative, and possibly spinning, target spacecraft. Most of existing work in the literature that address the problem of uncooperative relative vision-based navigation assume the existence of a CAD model of the unknown object. For example in [6] the algorithm used stereo camera and 3D model matching, Then applying matching algorithm called iterative closest point (ICP), in order to match Existing 3D model to 3d measurement point obtained from stereo matching, and uses time series of images to increase the reliability of the relative attitude and position estimates. In [7] the ICP algorithm implemented to register range data and model from stereo camera. In [8] stereo image of satellite model with white mat surface on the model took and the ICP algorithm was applied to matched known model to measure data points. Geometric Probing combining a voxel template set and a binary decision tree has been proposed to improve the weakness of ICP of potentially falling into a local minimum depending on the initial relative attitude between the model and measured data [9].

However, this method is suitable when prior knowledge about the geometry of the satellite is available, without such knowledge, the problem become more difficult. Another disadvantage of ICP algorithm is convergence to false local minima. Tomashi et al. [10] developed a factorization method. This method takes multiple images taken by monocular camera to measure the pose. But it also requires prior knowledge, such as the shape and dimension or the proportional dimension of the satellite. In addition, when the pose parameter is calculated, solutions of nonlinear equations will be involved, which makes computation more complicate. A vision-based relative navigation and control strategy for inspecting an unknown an, no cooperative object in space using a stereo camera proposed by Fourie et al [11]. The navigation system was based on image processing algorithms and a simple control approach was used to ensure that the desired range during the inspection maneuver. Proposed method have been implemented on VERTIGO Goggles hardware and experimentally validated on ISS Expedition 34. Our work is extended of their work.

In this paper, a vision-based relative navigation system applicable for non-cooperative spinning target using only a stereo gray scale camera is proposed. Compared to other sensors technologies, a camera-based system is energy-efficient, lightweight, and provides high information gain. The navigation system is based on image processing algorithms, which extract the relative position and velocities between the inspector and the target spacecraft. The primary contribution of our relative navigation system is its simplicity. The main benefit of this simplicity is having very low computational cost if implemented correctly; as a result, this relative navigation can be used with a very low power embedded computer. This paper is organized as follows: Section II provides a description of the image processing strategy used to determine the relative position between two spacecrafts. Section III describes the test-bed facility along with the stereo cameras. An evaluation and performance from laboratory experiments will be described in section IV. Section V closes the paper with a conclusion.

2. RELATIVE NAVIGATION APPROACH

2.1. Image Processing Algorithm

The proposed relative navigation approach intends to obtain relative position of unknown and spinning target based only on visual information from stereo cameras. At first raw stereo images were captured; however, for observing a spinning object; both stereo cameras must be precisely synchronized to capture images at the same time. In addition, the exposure time must be set low enough to minimize motion blur effect. To remove any lens distortions adjust for any misalignment between the lenses, as well as between the two image sensors themselves calibration is an important and essential step. This step was done by using the OpenCV library [12].

A significant amount of research has been done in the development of different algorithms for feature detection and matching over the last decades [13]-[15]. Two of the more well-known techniques that are invariant to scale and rotation are the so-called Scale Invariant Feature Transform (SIFT) [16] and Speeded Up Robust Feature (SURF)[17]. The SURF [17] descriptor was chosen as it has proved to be highly efficient in terms of scale-invariance and rotation, while being highly robust against several deformations. Additionally, the SURF method has the ability for real-time applications as a result of using integral images and box filters. Fig. 1 shows our strategy for motion measurement. To find relative motion it is required to compute disparity map of objects from a set of images. The position of the pixels in the left image to output the corresponding pixel location in the right image, from these information the disparity map can be computed, in which points closer to the camera are almost white whereas points further away are almost black. Points in between are shown in gray scale, which get darker as objects go further away. The disparity mapping here is produced by using a block matching algorithm known as the Sum of absolute differences (SAD). This is achieved by taking a square window of certain size around the pixel of interest in the reference image and finding the homologous pixel within the window in the target image, while moving along the corresponding scanline. Specifically, given an image (in which each pixel (u, v) corresponds to a projection of a threedimensional point onto camera focal plane) has a grayscale intensity value $I(u, v)$, an error function can be computed as:

$$\Phi_{SAD}(u,v) = \sum_{x=-M_1}^{M_1} \sum_{y=-M_2}^{M_2} \mid I_L(u+x+d, u+y) - I_R(u+x, u+y) \mid \quad (1)$$

Where $(2M_1 + 1) * (2M_2 + 1)$ is the size of matching window. I_L is the intensity of a pixel in the reference camera image in our case left camera and I_R is the intensity of corresponding pixel in right camera image and d is the disparity, i.e., the position difference of a given pixel. This value must then be optimized by minimizing the SAD error function. In the block matching method Selection of block size is a trade-off between depth-map noise and detail.

In addition to block matching algorithm ,the algorithm developed by Geiger [18], Library for Efficient Large-scale Stereo Matching(Libelas) was also used to compute disparity map from two rectified stereo pairs. This algorithm uses belief propagation with a prior obtained using the Delaunay triangulation of matched Sobel features to compute a global disparity map with a relatively low computational cost [11]. The block-matching algorithm used here has generally better performance than Libelas as we it was tested in dark room under high illumination, the dept map from Libelas was not accurate enough. This block-matching algorithm is known to yield good performance, and the confidence estimate can be used to effectively mask out regions of high noise. Selection of block size is a trade-off between disparity map noise and accuracy.

2.2. Coordinate System Rigid Body Motion Estimation From Image Sequences

The Distance between the observers (i.e., two cameras composing the stereo vision system) and the target satellite can be computed using the dense stereo approach.

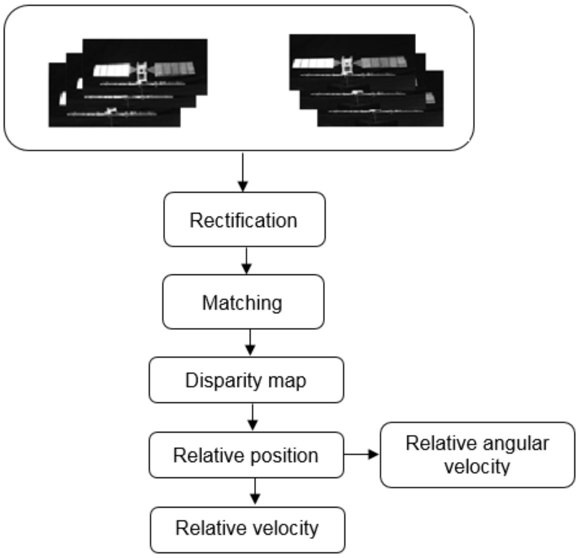

Figure 1: Proposed image processing algorithm.

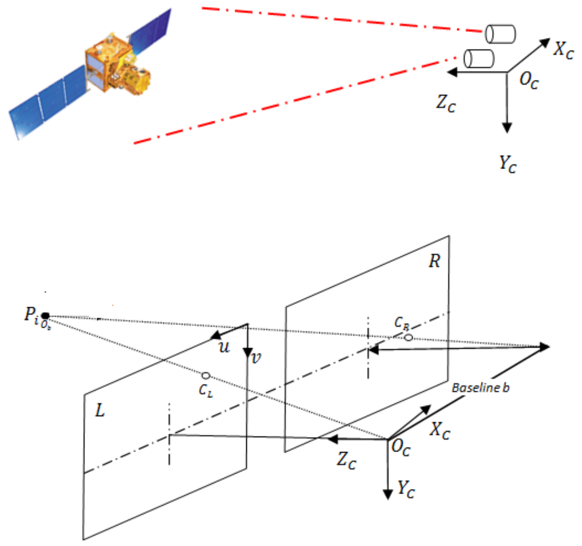

Figure 2: Geometrical relationship and coordinate systems

Dense stereo combines the two images obtained from the rectification process and to estimate the relative position between camera and spacecraft, related coordinate frames are needed. The measurement information of stereo vision system is described in stereo vision-fixed coordinate system. This coordinate system summarize as follow

- Camera frame $O_c - x_c y_c z_c$: a Cartesian right-hand body-fixed reference frame attached to the left camera. The origin of stereo vision-fixed coordinate system lies in the stereo vision system. It's z_c axis is parallel with the optical axis of the cameras, x_c is vertical to the optical axis, and the direction of axis y_c obeys the right-hand role. To be convenient, it is assumed that the camera frame and the chaser spacecraft body frame is the same one thus the measurement information of stereo vision system is described in this coordinate system.

- Image Frame $(F_I - uv)$: defined as a $2D$ frame on the image plane. Its u-axis and v-axis are in the direction of image horizon and vertical, respectively. O_I is the center of the image plane, and its coordinate is (u, v).

C_R and C_L are projection of the 3D point on the image plane of the right and left camera respectively. The rotation matrix and the translation vector between stereo vision-fixed coordinate system and target Body- can be acquired by calibration. The vector $P_i = [X_i, Y_i, Z_i]$ $^T \in R3$ denotes the position of pint P_i relative to the center Camera Frame O_c.

2.3. Rigid Body Motion Estimation From Image Sequences

The Distance between the observers (i.e., two cameras composing the stereo vision system) and the target satellite can be computed using the disparity map. Once the disparity map is computed, the points are triangulated to compute a three-dimensional point cloud. The measurement information of stereo vision system is described in stereo vision-fixed coordinate system.Fig. 2 graphically summarizes these frames. As is shown in fig.2, the stereo rig system composed of two parallel and aligned cameras, pointed at the target. Reconstructing 3D points are given as follows

$$Z = T_x * f/u - v \tag{3}$$

$$X = C_x - u * Z/f \tag{4}$$

$$Y = v - C_y * Z/f \tag{5}$$

Where f is the focal length, and C_x, C_y are the principal point coordinates in pixels and u, v are projection of 3D point onto camera pixel coordinate. Once 3-D point is computed, the mean value of this 3-D point is calculated and used as the estimate for the geometric center of the target object. An example of the result of implementing the stereo vision algorithm to the RADARSAT-1 model shown in Fig. 4 . The left image shows the original image from the left camera, whereas the right-hand image shows the threshold stereo disparity map, the green dot is at the location of the geometric center, and the position of this point, in centimeter, is shown as green text overlaid on the left-hand image. Note that these measurements represent the relative position between the geometric center of the object and the origin of a reference frame centered at the focal point of the left camera.

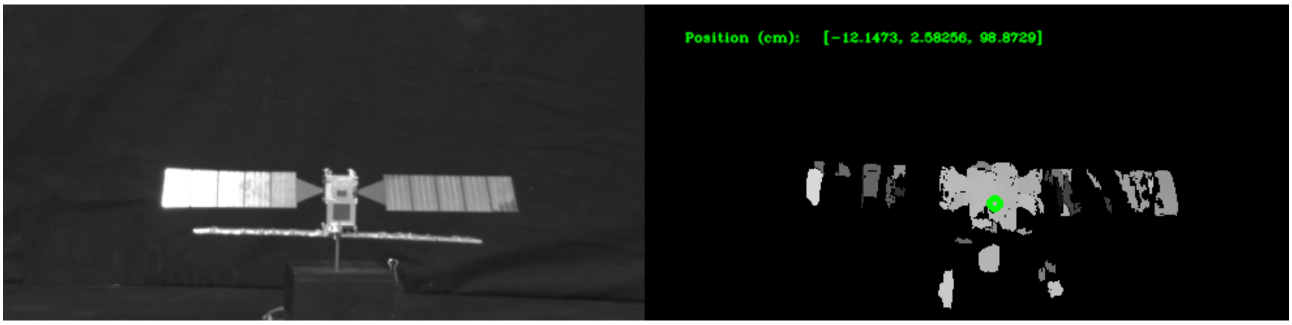

Figure 3: Stereo disparity map.

Table 1: The uEye UI-1220LE camera

Sensor	CMOS	Connection	USB 2.0
Shutter	Global	Optical Class	1/3”
Frame rate	87.2 fps	Resolution	752 x 480
Pixel format	8 bit		

3. LABORATORY TEST-BED

A laboratory test-bed emulating realistic on-orbit lightning conditions was developed to experimentally validate the vision-based techniques proposed in this work. This dark-room facility consists of a pair of calibrated and synchronized stereo monochrome ueye cameras which fixed side-by side with parallel lines-of-sight set 80 mm apart (the base line distance). The table 1 show the specification of Ueye camera. A scaled RADARSAT-1 Earth-observation spacecraft model attached to the shaft of a DC motor, hence emulating a major-axis spin. The rotational speed of the high-gear ratio motor can be controlled between 1 and 10 RPM through an Arduino computer. Two USB cameras are connected to a compute, in real-time, the relative state vector of the rotating satellite. Because the model spacecraft does not have any fiducially markers, this setup is representative of an autonomous inspection maneuver with a non-cooperative spinning target. Moreover, the body of the spacecraft model is manufactured from highly-reflective and specular wavy Multi-Layer Insulation (MLI) material with tinted mirrors for solar panels, thereby rendering relative navigation process do challenging. A light source simulating directional illumination is also employed, with the result that optical features significantly change depending on the lighting direction.

Using the technique described in the previous section, three dimensional relative position was determined, and the results are provided in Figs.1 and 2, for a stationary and a spinning target spacecraft at distance 0.64 m along the line-of-sight axis, where the solid lines represent measurement from stereo cameras along X,Y, Z, while and dotted lines correspond to real distance from tape measurement along again along X,Y, Z axes. Fig. 3 and Fig. 4 indicated absolute errors in position along X,Y, Z axis

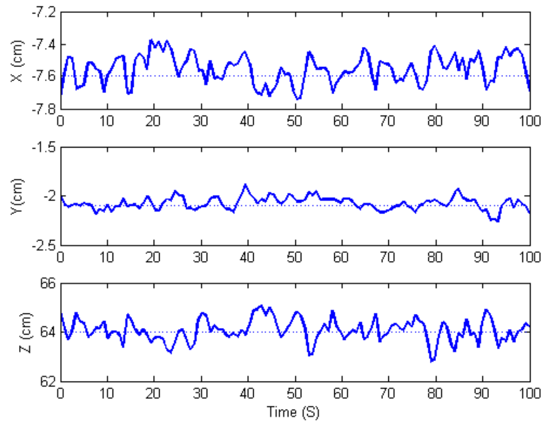

Figure 4: Relative position for a stationnary target.

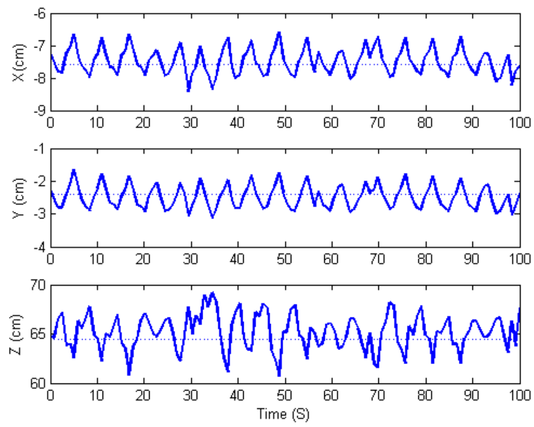

Figure 5: Relative position for a spinning target.

for a stationary and a spinning target spacecraft, respectively. Note that these error signals were generated by comparing the outputs of the relative vision-based navigation system with ground truth data obtained with a tape measure. As shown in these figures, the maximum position determination errors along each axis are less than 0.02 m for stationary and less than 0.05 m for spinning case , respectively. Another experiment was performed to assess the performance at varying distances along the line-of-sight axis, the relative position was determined at three arbitrarily distances: 0.47, 0.88, and 1.16 m. the relative position error for all above measurement was remind very low.

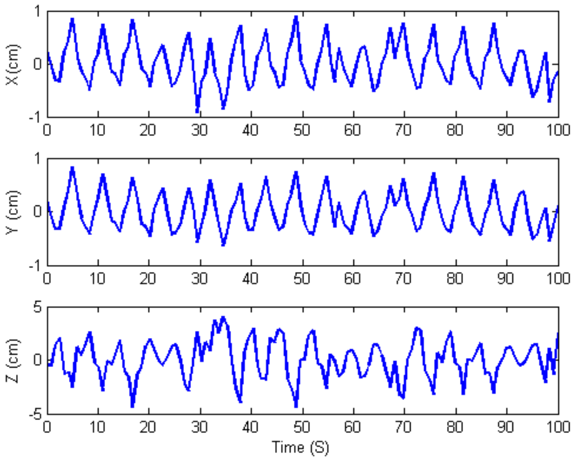

Figure 6: Relative position error for a spinning target.

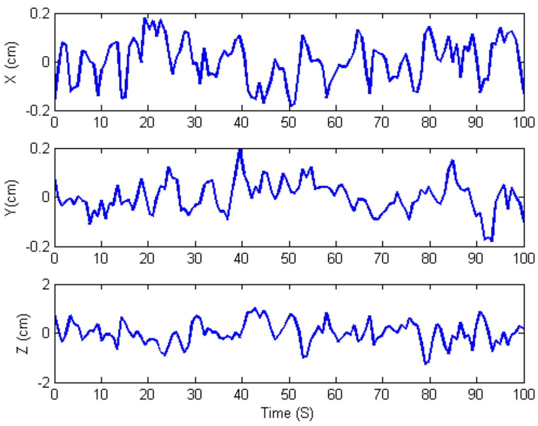

Figure 7: Relative position error for a stationnary target.

4. CONCLUSIONS

In this paper, a simple and very fast strategy was proposed for determining the relative position, between a chaser and an unknown spinning target spacecraft based only on calibrated stereo grayscale cameras. The proposed solution used the Speeded Up Robust Feature algorithm to extract and match features points between the two cameras. Then, a three-dimensional stereo disparity was calculated from which the relative position and was obtained. To simulate the on-orbital optical environment, a scaled satellite model with highly reflected material, a light source simulating the sun illuminates, and a stereo camera are employed in the test bed in order to evaluate the algorithm for real time application. Experimental results demonstrated that the simple uncooperative relative navigation system is applicable for real-time operations that require accurate performance. As future work, the development of a robust stochastic filter for obtaining the complete relative state vector (including the relative pose) with respect to an uncooperative spinning target will be investigated.

ACKNOWLEDGMENTS

The authors gratefully acknowledge the Canadian Space Agency for providing the CAD model of the RADARSAT-1 satellite from which the 1/50th scale model used in this work was built. The technical contributions from Jack Vedelago from Carleton University in the development of the testbed are also acknowledged.

REFERENCES

[1] Tarabini, L., Gil, J., Gandia, F., Molina, M. A., del Cura, J. M., and Ortega, G., Ground Guided CX-OLEV Rendez-Vous with Uncooperative Geostationary Satellite. Acta Astronautica, Vol. 61, No. 1, 2007, pp.312- 325.

[2] Lyn, C., Mooney, G., Bush, D., Computer Vision Systems for Robotic Servicing of the Hubble Space

Telescope, AIAA SPACE Conference , AIAA, Reston, VA, 2007; AIAA Paper 2007-6259.

[3] Romano, M., Friedman, D. A., and Shay, T. J., Laboratory Experimentation of Autonomous Spacecraft Approach and Docking to a Collaborative Target, Journal of Spacecraft and Rockets, Vol. 44, No. 1, 2007, pp. 164- 173.

[4] Tweddle, B. E., and Saenz-Otero, A., Relative Computer Vision-Based Navigation for Small Inspection Spacecraft, Journal of Guidance, Navigation, and Control, doi: 10.2514/1.G000687.

[5] MacLean, S. G., and Pinkney, H. F. L., Machine Vision in Space, Canadian Aeronautics and Space Journal, Vol. 29, No. 2, 1993, pp. 63- 77.

[6] Flores-Abad, A, Ma, O., Pham, K., and Ulrich, S., A Review of Space Robotics Technologies for On-Orbit Servicing, Progress in Aerospace Sciences, Vol. 68, 2014, pp. 1-26..

[7] Fuyuhito, T. , Kamimura, H., and Nishida, S., Motion Estimation to a Failed Satellite on Orbit Using Stereo Vision and 3D Model Matching, 9th International Conference on Control, Automation, Robotics and Vision, Inst. of Electrical and Electronics Engineers, Piscataway, NJ, 2006, pp. 1-8.

[8] Fuyuto, T., Model Based Visual Relative Motion Estimation and Control of a Spacecraft Utilizing Computer Graphics, 21st International Symposium on Space Flight Dynamics, Tolouse, France, 2009.

[9] Jasiobedzki, P., Greenspan, M., and Roth, G., Pose Determination and Tracking for Autonomous Satellite Capture, International Symposium on Artificial Intelligence and Robotics , Canada, June 18-22, 2001.

[10] Tomasi, C., and Kanade, T., Shape and Motion from Image Streams Under Orthography: A Factorization Method, International Journal of Computer Vision, Vol. 9, No. 2, 1992, pp. 137-154.

[11] Fourie, D., Tweddle, B. E., Ulrich, S., and Saenz-Otero, A., Flight Results of Vision-Based Navigation for Autonomous Spacecraft Inspection of Unknown Objects, Journal of Spacecraft and Rockets, Vol. 51, No. 6, 2014, pp. 2016-2026.

[12] Bradski, G., and Kaehler, A., Learning OpenCV: Computer Vision with the OpenCV Library, OReilly, Cambridge, MA, 2008.

[13] Cyganek, B. and Siebert, J. P., An Introduction to 3D Computer Vision Techniques and Algorithms, Wiley, 2009.

[14] Rublee, E., Rabaud, V., Konolige, K., and Bradski, G., ORB: An Efficient Alternative to SIFT or SURF, IEEE International Conference on Computer Vision, Inst. of Electrical and Electronics Engineers, Piscataway, NJ, 2011, pp. 2564-2571.

[15] Stockman, G., and Shapiro, L. G., Computer Vision, Prentice Hall, Upper Saddle River, NJ, 2001.

[16] Lowe, D. G., Object Recognition from Local Scale-Invariant Features, IEEE International Conference on Computer Vision, Inst. of Electrical and Electronics Engineers, Piscataway, NJ, 1999, pp. 1150-1157.

[17] Bay, H., Ess, A., Tuytelaars, T., and Van Gool, L. SURF: Speeded Up Robust Features, Computer Vision and Image Understanding, Vol. 110, No. 3, 2008, pp. 346-359.

[18] Geiger, A., Roser, M., and Urtasun, R., Efficient Large-Scale Stereo Matching, Computer Vision ACCV 2010, Part 1, Lecture Notes in Computer Science, Springer-Verlag, Berlin, Heidelberg, Vol. 6492, 2011, pp. 2538.